

HYDRATED SULFATES IN THE SYDNEY COALFIELD, CAPE BRETON, NOVA SCOTIA*

ERWIN L. ZODROW

*Research Associate of the Nova Scotia Museum, Halifax, and Department of Mathematics
and Natural Sciences, College of Cape Breton*

KEITH McCANDLISH

*Department of Mathematics and Natural Sciences, College of Cape Breton, Sydney,
Nova Scotia B1P 6J1*

ABSTRACT

Hydrated sulfates associated with decomposition of pyrite and copper-iron sulfides occur in coal in contact with the atmosphere. Melanterite, rozenite, epsomite, pickeringite, halotrichite, aluminocopiapite and sideronatriite were identified from coal seams and mines in the Sydney coalfield. This is apparently the first reported occurrence of sideronatriite and aluminocopiapite in North America, and for the remaining minerals with the possible exception of melanterite, first occurrences from Cape Breton. Crystallization of melanterite, and possibly of other hydrated sulfates, contributed substantially to the mechanical instability of coal faces in old underground workings by erosion of supporting pillars. In addition, alunite, jarosite, natrojarosite and barite (?) were tentatively identified from the Evans coal mine situated in a Carboniferous basin somewhat older than the Sydney basin. These sulfates are associated with the decomposition of copper-iron sulfides and possibly pyrite. All minerals were identified by X-ray powder diffraction.

SOMMAIRE

On trouve des sulfates hydratés résultant de la décomposition de pyrite et de sulfures de Cu-Fe dans le charbon exposé à l'air. Mélanterite, rozenite, epsomite, pickeringite, halotrichite, aluminocopiapite et sidéronatriite ont été identifiées (par clichés de poudre) dans les couches de charbon des mines du bassin houiller de Sydney. C'est la première découverte de sidéronatriite et d'aluminocopiapite en Amérique du Nord; quant aux autres minéraux, sauf peut-être la mélanterite, c'est la première fois qu'on les trouve au cap Breton. La formation de la mélanterite, et peut-être aussi celle des autres sulfates hydratés, a grandement contribué à l'instabilité des fronts de taille, par érosion des piliers de soutènement, dans les anciens chantiers souterrains. De plus, alunite, jarosite, natrojarosite et barite(?) ont été identifiées pro-

visoirement dans la mine Evans, située dans un bassin houiller carbonifère plus ancien que celui de Sydney. Ces sulfates sont des produits de la décomposition de sulfures de Cu-Fe et peut-être aussi de pyrite.
(Traduit par la Rédaction)

PYRITE IN COAL

An investigation of occurrences and patterns of distribution of hydrated sulfate minerals constitutes the first phase of a proposed environmental study program. The overall purpose of the investigation is to identify and define water pollutants associated with oxidation of pyrite in exposed coal seams, producing mines, and in coal piles stored in the open air. Pyrite is a ubiquitous mineral in the coal seams of the Sydney coalfield.

The Sydney coalfield, situated on the north-eastern part of Cape Breton, forms the south-eastern border of a deformed basin assumed to be of Carboniferous age (Bell 1938). The basin trends northeast into the Atlantic Ocean. Coal measures in the basin outcrop along the Atlantic coast in an east-west belt, but synclinal-anticlinal structures on-shore modify this trend, locally quite substantially. Bell (1938) divided the Sydney coalfield into three distinguishable zones using assemblages of fossil flora, *i.e.*, fern-like and fern-type fossils. All coal mines in this basin exploit coal measures that belong to the youngest zone, which may be equated with the Upper Pennsylvanian. The Lingan mine and the 1-A mine in #26 Colliery exploit the Harbour seam, and the Prince mine at Point Aconi, the Stubbart seam (Fig. 1). However, sampling has not been restricted to these seams.

Fine-grained pyrite in the coal measures of the Sydney coalfield originated in peats of Pennsylvanian age; however, structural studies indicate that coalification of the peat took place much later. Pyrite mineralization in coal is pos-

*Contribution from the Nova Scotia Museum, Halifax, N.S.

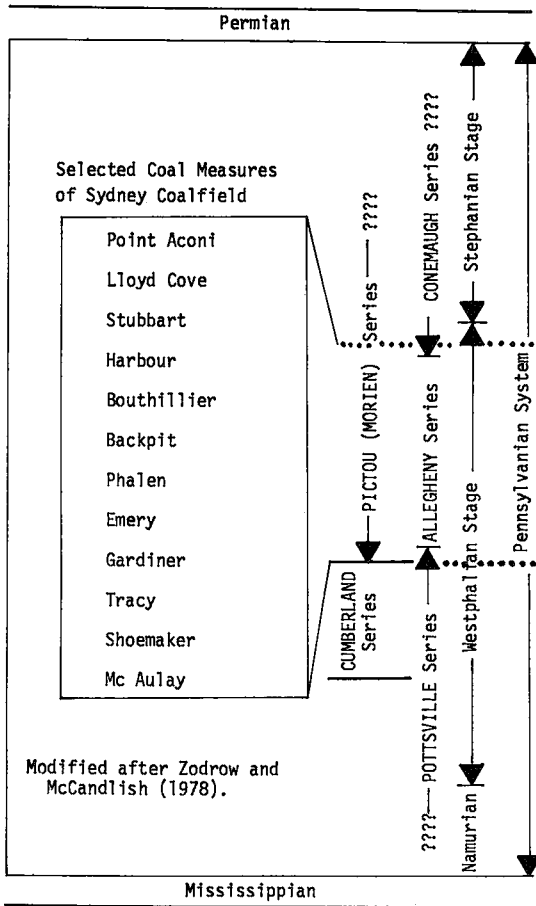


FIG. 1. Coal measures of Sydney coalfield in approximate correlation to the Pennsylvanian series of Nova Scotia (Cumberland to Morien), Pennsylvania (Pottsville to Conemaugh), and Europe (Namurian to Stephanian).

sibly derived from ester sulfates, hydrocarbon sulfates that originate from biogenic sources (Casagrande & Siefert 1977). Concentrations of ester sulfates are much greater in marine than in fresh-water peat.

Selected pyrite samples were examined by optical methods and by X-ray powder diffraction analysis (XRD). Preliminary results show traces only of marcasite in sample 977GF-58 (accession and catalogue number of the Nova Scotia Museum) from the McAulay seam. In samples 977GF-176, F-177, and F-178 from the Phalen seam (Fig. 2), polished sections (Fig. 3) show that pyrite is present in the coal a) as nodules with apparently unstable cores, and b) between veins of nodules as elongate crystals aligned perpendicular to the veins. In the second case

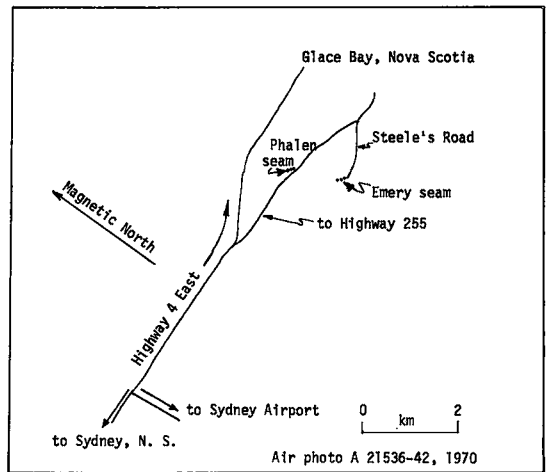


FIG. 2. Location map for the Phalen and Emery seams near Glace Bay, Cape Breton, N.S.

the original marcasite has apparently been transformed to pyrite.

The Stubbart seam exploited in the Prince mine contains two conspicuous fine-grained pyrite bands; these may be traced over a wide area in the mine. They are irregular in thickness (pyrite specimen 977GF-622 is approximately 4 cm thick), locally nodular and discontinuous. Specimens of hydrated sulfates collected underground in the Prince mine occur in these two bands. In addition pyrite may occur in radiating rosette-type structures less than 6 cm across (977GF-243), and in isolated nodules of 3 to 5 cm (977GF-205). As a replacement of plant tissue, pyrite plays only a minor role, but in specimen 977GF-244 it replaces a stigmairian structure (root system of either *Lepidodendron* or *Sigillaria* species). Locally replacement of foliage of arborescent plants of the type *Lycopodites meekii* Lesquereux (977GF-97b) or *Lepidodendron dawsoni* Bell also occurs.

In the Phalen seam at the 1-B mine of #26 Colliery in Glace Bay, pyrite is disseminated in the coal, and hence hydrated sulfate minerals are distributed throughout this seam. In outcrops of the seam (Fig. 2) pyrite may be concentrated in bands or nodules; specimen 977GF-177 furnishes an example of nodular pyrite. The presence of pyrite in coal seams, however, is not a guarantee that hydrated sulfates have formed; certain pyrite specimens show no evidence of sulfate formation.

ANALYTICAL TECHNIQUES

XRD techniques were used in all identifica-



FIG. 3. Infrared reflection image of elongate crystals of pyrite perpendicular to the veins (x8); 977GF-177 Negative.

tions of sulfates; these were supplemented by qualitative chemical analyses and optical examination in specific cases. Melanterite and rozenite (977GF-653-2) were identified by comparison with Powder Diffraction File (PDF) 1-225 and 16-699, respectively; pickeringite (977GF-682-1) was compared to PDF 12-299. These minerals were exposed to Ni-filtered $\text{CuK}\alpha$ radiation in a 57.3 mm Debye-Scherrer camera. Sideronatrite (977GF-653-1) and epsomite

(977GF-653-3) were exposed to Fe-filtered $\text{CoK}\alpha$ radiation in the same camera, except that a 114.6 mm film of sideronatrite was also made. Epsomite was identified by comparison to a standard film, whereas sideronatrite was identified by comparison with PDF 17-156, and with a standard pattern at the Geological Survey of Canada (pers. comm. L. J. Cabri 1977).

Samples 977GF-691 and 977GF-704 from the Evans Mine at St. Rose, Cape Breton, were exposed to Ni-filtered $\text{CuK}\alpha$ radiation (pers. comm. M. Zentilli 1977); samples 977GF-682-2 and 977GF-682-1-1 were exposed to $\text{CoK}\alpha$ radiation with an Fe-filter (pers. comm. J. K. Sutherland 1977).

HYDRATED SULFATES AT 1-B MINE, GLACE BAY

Co-existing in the Phalen seam (Fig. 4) are melanterite, sideronatrite, and epsomite. Melanterite, $\text{FeSO}_4 \cdot 7\text{H}_2\text{O}$, is the name given to the species wherever $\text{Fe} > \text{Cu}$. Melanterite occurs throughout the coal face and crystallized perpendicular to it as falcate fibres up to 3 cm long, and within the coal as oval-shaped, fibrous masses generally less than 5 cm long. Crystal growth of melanterite and other hydrated sulfates is directly responsible for fragmentation of coal faces, which leads to progressive mechanical erosion of supporting pillars. Indeed, the stress necessary for the mechanical erosion of coal is supplied by the oxidation of pyrite and

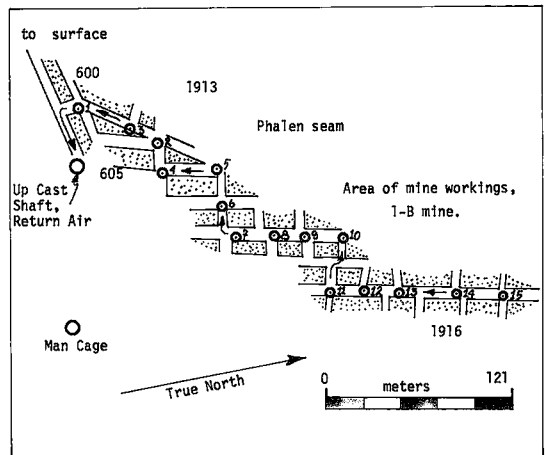


FIG. 4. Part plan of the 1-B mine, #26 Colliery, Glace Bay, N.S. showing numbered sample locations. Elevations (in feet) below sea level. Arrows indicate return air flow (to the surface). Roof-support pillars from mining activity (1913 to 1916) are shown as stippled areas.

attendant volume increases that occur to produce hydrated sulfates. Crosscuts driven sixty years ago now have a V-shaped appearance due to accumulation of melanterite-bearing coal detritus. Roofs consist of shales or shaly sandstone in which the fossil plant content is high; in addition, the growth of sideronatrite, epsomite and other unidentified non-metallic minerals may lead to weakening, then roof collapse. The fossil plants most detrimental in this context are large sigillarian trees, now compressed, and their abundant reed-like foliage. The carbon remains of this fossil material created planes of weakness in the sandstone; similar comments apply to selected roof zones in the Prince mine, where the most detrimental fossil to roof stability is *Calamites carinatus* Sternberg (977GF-245), herbaceous reed-like plants several meters long. However, as these old mine workings show, the size of the fallen slabs is largely dependent on enlargement of rooms by erosion of pillars.

Table 1 summarizes values of relative humidity and temperature of return air (ventilation) at which melanterite is found in the 1-B mine; no inference can be made from this tabulation concerning the lower limits of melanterite stability. The temperature and humidity of the air returning to the surface are constant and independent of surface atmospheric conditions; air pressure in the mine is directly under the influence of surface air pressure.

Experiments in our laboratory indicate that melanterite is stable in an atmosphere having a relative humidity as low as 60% at 25-28°C. The tetrahydrate rozenite, $\text{FeSO}_4 \cdot 4\text{H}_2\text{O}$, was obtained from melanterite specimens by dehydration in atmospheric conditions. However, it is not entirely clear whether the tetrahydrate can be formed without passing first through the heptahydrate stage, melanterite. Determination of optic signs of melanterite from various sample sites (Fig. 4) shows that the angle $2V$ lies close

to $\pm 90^\circ$; this compares to 80° in Mason & Berry (1968), and $85^\circ 27'$ for synthetic melanterite in Na light (Palache *et al.* 1951). Variability in the optic sign implies variability in the composition of melanterite. This conjecture may be supported by difference in color of specimens roughly equal in thickness, from greenish-blue to straw-yellow to white; impurities, of course, may also cause color changes. Variation in the composition of melanterite may reflect sample location; this aspect has not been investigated.

Sideronatrite, $\text{Na}_2\text{Fe}(\text{SO}_4)_2(\text{OH}) \cdot 3\text{H}_2\text{O}$, is bright lemon yellow and occurs as a fibrous crust on coal; it is stable in surface conditions. Because of their similar colors, sideronatrite and jarosite may be confused. Qualitative wet chemical analysis indicates the presence of phosphate, chromate, and possibly Ni, Al, and Mg in our sideronatrite samples (977GF-653-1). Under the polarizing microscope, parallel extinction can be easily observed due to the excellent cleavage on {100}. Since the discovery of this mineral in the Sydney coalfield, we suspect that many mineral specimens tagged as jarosite are actually sideronatrite. This applies especially to the roofs of various working areas of the Prince mine and the 1-B mine.

The only location of sideronatrite known to the authors is in the 1-B mine. At samples sites 1 and 7, Figure 4, sideronatrite "mushrooms" out of the coal face in patches parallel to the bedding planes. Flecks of a yellow mineral are visible throughout the coal faces along the travel road (escape drift to surface); the mineral is assumed to be sideronatrite. Yellow material also coats fossil plants, especially *Sigillaria*, that are preserved in the syringodendron condition (977GF-625, F-627).

Epsomite, $\text{MgSO}_4 \cdot 7\text{H}_2\text{O}$, is white and fibrous; the fibres attain 3-4 cm. Epsomite cannot be confused with rozenite because of their different modes of origin and crystal habits. Epsomite is highly localized in the roof of the Phalen seam and occurs with quartz; an inverse correlation is observed between the occurrence of epsomite and melanterite. Epsomite was not observed on coal faces. Therefore, we conclude that this seam did not carry sufficient quantities of magnesium to form the mineral. The 1-B mine provides the only occurrence of this mineral known so far. The collection sites include 5, 6 and 10 (Fig. 4), where the mineral was collected from slabs of sandstone caved in from the roof.

Hoffmann (1890) was the first to report melanterite and epsomite in Nova Scotia (Traill 1970); he found melanterite on shale of mined coal in Glace Bay, and epsomite in a gypsum quarry in Hants County.

TABLE 1. AIR TEMPERATURE ($^\circ\text{C}$) AND RELATIVE HUMIDITY (%) FROM HYGROMETRIC DATA ALONG THE TRAVEL ROAD IN 1-B MINE, GLACE BAY, N. S.

Sample Site	$T^\circ\text{C}$	R.H.%	Sample Site	$T^\circ\text{C}$	R.H.%
1	15.9	90	9	15.5	81
2	15.5	90	10	15.5	81
3	15.4	90	11	15.8	81
4	15.5	81	12	15.8	81
5	15.8	81	13	15.3	81
6	15.7	81	14	15.5	90
7	15.5	81	15	15.1	90
8	15.5	81			

HYDRATED SULFATES AT THE PRINCE MINE, POINT ACONI

Melanterite and rozenite are the hydrated sulfates that have been identified from this mine. Rozenite, $\text{FeSO}_4 \cdot 4\text{H}_2\text{O}$, is white and powdery, and readily soluble in water as is melanterite. Some optical and chemical data relating to rozenite are given by Jambor & Traill (1963). This mineral is stable over a large range of fluctuating atmospheric conditions. Our investigation into sulfate mineralization was confined to areas about 450 m from surface entrances of adits #4 and #5. In this area humidity and temperature conditions are dependent in part on atmospheric conditions at the surface. Relative humidity recorded on 28th September 1977 was between 90 and 98% and the fresh-air temperature between 12.1 and 16.8°C. As a result of variation of humidity and temperature in this area, melanterite growth is not spectacular, and is restricted to short fibres in small quantities; therefore, mechanical erosion of the coal faces is hardly noticeable.

Melanterite and rozenite are believed to co-exist in these two adits; however, a phase equilibrium study would be necessary to check this preliminary hypothesis. Rozenite is also observed on surface outcrops of the Stubbart seam (977GF-660). Rain water that percolated through coal storage piles has a low pH value of about 2.0; bacterial activity is believed to aid in the breakdown of pyrite.

Pyrite specimen 977GF-655-1 continues to grow melanterite crystals (+ rozenite?) in a hermetically sealed glass container stored in our laboratory. The relative humidity in the container is kept at about 90%. However, additional XRD data are needed to confirm that rozenite is growing directly on the pyrite without passing through the heptahydrate stage. A 28 by 15 cm pyrite specimen (977GF-622) collected from a coal storage pile and now stored in atmospheric conditions in the laboratory is developing fracture planes; we believe that these are due to the growth of a fine-grained whitish, unidentified material.

HYDRATED SULFATES, SULFATES, SULFIDES, AND CARBONATES AT OTHER LOCATIONS ON CAPE BRETON ISLAND

Rozenite occurs also in minor quantities in outcrops of the Phalen seam in Glace Bay (Fig.

2), where it is visibly associated with fine-grained pyrite (977GF-177). Pickeringite, $\text{MgAl}_2(\text{SO}_4)_4 \cdot 22\text{H}_2\text{O}$ (977GF-682-1), alunocopiopite, $\text{MgAlFe}(\text{SO}_4)\text{OH} \cdot \text{H}_2\text{O}$ (977GF-682), and halotrichite, $\text{FeAl}_2(\text{SO}_4)_4 \cdot 22\text{H}_2\text{O}$ (977GF-682-1-1) coexisted in surface outcrops of the Emery seam; heavy rains have since obliterated these water-soluble minerals.

The Evans coal mine, situated in an Upper Carboniferous basin near the town of Inverness, exploits the #5 coal seam. Typical fresh-water fauna, *Anthraconaia cf. modiolaris*, a pelecypod, and *Carbonita fabulina*, an ostracod (977GF-696, F-697, respectively) occur in the roof of this coal seam. The faunal association can be directly correlated with that of the Lower Coal Measures of Great Britain: Westphalian A, early B, *i.e.*, older than the strata of Sydney coalfield (Copeland 1977). Preliminary interpretation of XRD data suggested the presence of barite and alunite, $\text{KAl}_3(\text{SO}_4)(\text{OH})_6$, in a discordant 2-5 mm vein cutting the upper contact between coal and overlying sediments (977GF-691); however, further analytical work is necessary on this specimen to confirm the presence of these minerals. Sample 977GF-704 and others originating from the top of the producing coal seam, #5, show evidence of gypsum and members of the jarosite-natrojarosite series in which Na substitutes for K: $(\text{K}, \text{Na})\text{Fe}_3(\text{SO}_4)_2(\text{OH})_6$.

The distribution and occurrence of hydrated sulfates and sulfides in the Evans coal mine are fundamentally different from those in the Sydney coalfield. In this mine all hydrated sulfates and sulfides are restricted to a 3-5 mm vein that contains bornite, chalcocopyrite, pyrite and other unidentified minerals. The vein, concordant with the coal seam and directly on top of it, is a tracer horizon in the mine and may indeed be an indicator of the #5 seam. However, hydrated sulfates occur only in those places where the sulfide vein has been exposed to the atmosphere for a number of years, and thus never along working faces. Indeed, no sulfates have yet been collected from these faces; this is also true for Prince mine, Lingan mine, and 1-A mine of #26 Colliery in the Sydney coalfield. The #5 coal seam has prominently developed joint planes perpendicular to the seam and trending along its strike; the planes are occupied by thin sheets of calcite (977GF-699); a similar situation exists in the Sydney coalfield (977GF-719). Calcite (977GF-700) was also identified from a very small stalactitic-type of structure on a coal face. Rozenite is also suspected at this mine but not yet identified.

DISCUSSION

Apart from having world-famous fossils of the type *Lonchopteris eschweiliana* Andrae (977GF-463), the coal mines of the Sydney coalfield show renewable hydrated sulfate minerals in their natural environments. As many of these salts are readily soluble in water, the occurrence of some of them is dependent on hot, humid weather conditions. Simple experiments in the laboratory show that fine-grained pyrite started to "grow" sulfates within three days after collection at ambient temperatures of about 25-28°C. However, the chemical process in the Sydney specimens did not take place if copper sulfides were present in addition to pyrite (977GF-308, F-382). We have collected only the obvious, but are convinced that many esoteric sulfates await discovery. The research needed for this investigation includes ore microscopy, to investigate the relationship between marcasite and pyrite, not only *vis-à-vis* oxidation to produce hydrated sulfates, but also in search of geochemical factors that played a temporal role in the coalification of the Pennsylvanian swamps. Thus elucidation of the origin of pyrite, and hence its distribution in the coal, would form a firm basis for environmental studies and the study of hydrated sulfates; geostatistical methods, such as oblique factor analysis (Zodrow 1976) are appropriate. Detailed optical and chemical data from collected samples may aid in fitting the empirical data to theoretically possible solid-solution series of the type alunite-jarosite-natrojarosite (Mason & Berry 1968) and to substitution schemes in sideronatrite and pickeringite as well.

Questions of environmental nature are also broached by this investigation: the role of bacteria in the formation of sulfuric acid in storage piles of coal, and spontaneous combustion *vis-à-vis* hydrated sulfate-mineral formation.

ACKNOWLEDGEMENTS

The Cape Breton Development Corporation (Devco) gave permission to publish part of the plan of the 1-B mine, and to collect at various underground mines. J. MacLellan, manager of Devco's #26 Colliery provided us with underground "guides" B. Morrison, who suggested investigating the travel road in 1-B mine for fossils, J. Nicholson and G. Crosby who watched us like hawks so that we would not stray from

the safe travel road in this mine. Similarly, D. Merner, manager of the Prince mine, supplied mine technologist G. Ellerbrok for our safety; we express our thanks.

Identifications of minerals by XRD were carried out by J. M. Stewart (1977) and L. J. Cabri (1977) of the Canada Centre for Mineral and Energy Technology, Ottawa, by M. Zentilli, Department of Geology, Dalhousie University and by J. K. Sutherland, Research and Productivity Council, Fredericton. The authors are also grateful to referees of the journal for pointed critique and suggestions contributing to improvement of the presentation. The authors gratefully acknowledge financial assistance from the College of Cape Breton (Grant CCB10058).

Note added in proof: Fibroferrite, $\text{Fe}(\text{OH})\text{SO}_4 \cdot 5\text{H}_2\text{O}$ has been identified in coal specimen 977GF-655-13, from the Stubbart seam at the Prince mine, Point Aconi.

REFERENCES

- BELL, W. A. (1938): Fossil flora of Sydney Coalfield, Nova Scotia. *Geol. Surv. Can. Mem.* 215.
- CASAGRANDE, D. & SIEFERT, K. (1977): Origins of sulfur in coal: Importance of the ester sulfate content in peat. *Science* 195, 675-676.
- COPELAND, M. J. (1977): Upper Carboniferous fresh-water fauna from the roof of #5 coal seam, St. Rose, Inverness. *Geol. Surv. Can., East. Paleont. Sect. Rep.* MP-9-1977-MJC.
- HOFFMANN, G. C. (1890): Annotated list of the minerals occurring in Canada. *Ann. Rep. Geol. Nat. Hist. Surv. Can.* 4, T1-67.
- JAMBOR, J. L. & TRAILL, R. J. (1963): On rozenite and siderotil. *Can. Mineral.* 7, 751-763.
- MASON, B. & BERRY, L. G. (1968): *Elements of Mineralogy*. W. H. Freeman & Co., San Francisco.
- PALACHE, C., BERMAN, H. & FRONDEL, C. (1957): *The Systems of Mineralogy* 2, 7th ed. J. Wiley & Sons, New York.
- TRAILL, R. J. (1970): A catalogue of Canadian minerals. *Geol. Surv. Can. Pap.* 69-45.
- ZODROW, E. (1976): Minres factor analysis of hypersthene data, Strathcona Mine (Ontario, Canada). *Math. Geol.* 8, 395-412.
- & McCANDLISH, K. (1978): Annotated catalogue of Carboniferous fossil plants of Nova Scotia in the collection of the Nova Scotia Museum, Halifax. *Nova Scotia Museum* (in press).

Manuscript received September 1977, emended November 1977.

TALNAKHITE AND MOOIHOEKITE: THE ACCESSIBILITY OF ORDERED STRUCTURES IN THE METAL-RICH REGION AROUND CHALCOPYRITE

A. PUTNIS

Department of Mineralogy and Petrology, University of Cambridge, Cambridge CB2 3EW, England

ABSTRACT

Phase transformations in natural talnakhite, and natural and synthetic mooihokite have been studied dynamically by *in situ* experiments in a transmission electron microscope. The talnakhite structure is a metastable transformation product formed under conditions in which the transformation to the more stable mooihokite structure is kinetically impeded. The relationship between talnakhite and mooihokite is described in terms of Time-Temperature-Transformation diagrams for the two phases. The nature of the transformations can be described theoretically using the symmetry-point ordering theory.

SOMMAIRE

L'étude dynamique des transformations de phase dans la talnakhite et la mooihokite (y compris la mooihokite synthétique) repose sur des expériences faites *in situ* au microscope électronique à transmission. La structure de la talnakhite est le produit métastable d'une transformation qui, cinétiquement, entrave le passage à la structure plus stable de la mooihokite. La relation entre talnakhite et mooihokite est illustrée par des diagrammes Temps-Température-Transformation pour les deux phases. Les transformations sont traitées selon la théorie de la mise en ordre des points de symétrie.

(Traduit par la Rédaction)

INTRODUCTION

At elevated temperatures, phase relations in the central part of the Cu-Fe-S system are dominated by the existence of an extensive solid solution in which the cations are disordered over the tetrahedral interstices of a cubic close-packed sulfur structure, space group $F\bar{4}3m$ (Cabri 1973). At low temperatures a number of ordered or partly ordered phases exists on the metal-rich side of stoichiometric CuFeS_2 . These phases, talnakhite ($\text{Cu}_9\text{Fe}_8\text{S}_{16}$), mooihokite ($\text{Cu}_9\text{Fe}_8\text{S}_{16}$) and haycockite ($\text{Cu}_4\text{Fe}_3\text{S}_8$) are considered to be stable phases with distinct stoichiometric compositions and well-defined structures (Hall & Gabe 1972; Cabri 1973; Hall & Rowland 1974; Rowland & Hall 1975; Hall 1975). Their structures are based on ordering of the extra cations

among the interstitial sites, giving rise to superstructures with a face-centred cubic subcell. Of particular interest here are talnakhite, with a $2a \times 2a \times 2a$ cubic supercell, space group $I\bar{4}3m$, and mooihokite with a $2a \times 2a \times 1a$ tetragonal supercell, space group $P\bar{4}2m$ (where a is the cell parameter of the subcell). Low-temperature phase relations are generally interpreted by considering these minerals as separate entities.

This paper is concerned with the route by which the high-temperature solid solution orders to form these phases, the constraints on the ordering processes and hence the relationship between partly ordered and ordered phases. Putnis & McConnell (1976) have shown that for a metal-enriched chalcopyrite with composition of the form $\text{Cu}_{1+z}\text{Fe}_{1+z}\text{S}_2$, the equilibrium behavior involves the formation of a tetragonal $P\bar{4}2m$ structure directly from the $F\bar{4}3m$ disordered solid solution. Under conditions of supercooling two metastable phases were formed. At temperatures slightly below the stable transformation temperature a $P\bar{4}3m$ phase with a cell edge equal to that of the solid solution was observed, and at a slightly lower temperature a modulated $I\bar{4}3m$ phase of cell dimension $2a$ was formed. These results were largely in agreement with Hiller & Probsthain (1956) who first suggested that the two phases equivalent to the $I\bar{4}3m$ and $P\bar{4}2m$ phases could be formed with the same composition. As these two phases have been equated with the naturally occurring minerals talnakhite and mooihokite, respectively (Cabri 1973), the question of the relationship between them arises, specifically in the light of the kinetically controlled behavior observed by Putnis & McConnell.

Natural assemblages of talnakhite and mooihokite and synthetic mooihokite were generously provided by Dr. L. J. Cabri; the ordering behavior of these materials could thus be compared with that of metal-enriched chalcopyrite. The processes relating to the formation of haycockite, also present in the material, will be discussed in a later paper.

EXPERIMENTAL TECHNIQUE

The talnakhite used in this study is from Noril'sk, western Siberia; the material and its associated intergrowths were described by Cabri (1967). The mooihoekite, from Mooihoek, Transvaal, occurs as an intergrowth with haycockite. This material has been described by Cabri & Hall (1972). The synthetic mooihoekite, specimen number 414 of Cabri (1973), is described as single-phase mooihoekite with bulk composition corresponding to $\text{Cu}_6\text{Fe}_9\text{S}_{16}$. Further details of the annealing treatment during synthesis are provided by Cabri (1973).

The natural minerals were analyzed with an energy-dispersive electron microprobe comprising a Si(Li) solid-state detector and Harwell pulse processor (Kandiah *et al.* 1975) interfaced to a Data General Nova 1220 minicomputer with 20K core storage. The results for talnakhite and mooihoekite, both apparently single-phase in reflected light, are shown in Figure 1. The results were calculated using a computer program employing the iterative spectrum stripping technique (Statham 1976). Relative accuracy of the results is estimated at $\pm 2\%$, and the precision of the analyses estimated at $\pm 1\%$ (relative). It would appear therefore that the scatter shown in Figure 1 is not spurious but reflects either

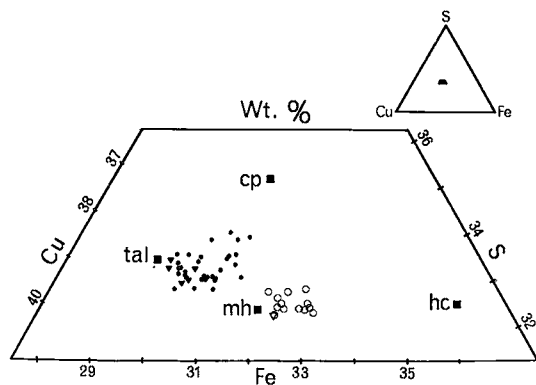


FIG. 1. Electron microprobe compositions of apparently single-phase (in reflected light) talnakhite from Noril'sk (closed circles) and mooihoekite from Mooihoek (open circles). The Ni contents (average 0.3 wt.% in mooihoekite and 0.7 wt.% in talnakhite) have been added to the Fe in this plot. The filled triangles are the 5 talnakhite analyses from Cabri & Harris (1971) and the open triangle is the average of 13 mooihoekite analyses from Cabri & Hall (1972). Electron microscope observations, however, show that apparently single-phase regions may be multiphase.

microstructural inhomogeneities in the sample or the possibility that the phases have a range of composition. The microstructures and the transformation behavior of the phases, described later in this paper, suggest that both may apply.

Samples of the minerals were crushed and the finest grains collected from suspension in absolute alcohol and mounted on a standard carbon-coated grid for observations in an AEI EM6G transmission electron microscope operating at 100 kV. After crushing, all material was kept in a vacuum to prevent tarnishing. More than 40 such mounts were prepared with material from different parts of the polished sections, and within each mount more than 100 grains were observed before and after heating, so that the results described here probably reflect an accurate sampling of the material.

The heating effect of the electron beam was used to induce the transformations in the grain under observation. A combination of focusing, defocusing and lateral shifts of the beam enables the temperature in the grain to be controlled precisely, although the inability to determine temperatures directly in these *in situ* experiments constitutes a limitation of the technique. The transformations were observed in a large number of grains in different orientations, providing detailed information on the crystallographic changes in the sample as a function of temperature. Any indication of bulk compositional change due to sulfur loss is immediately obvious as a surface degradation of the grain, and the results presented here describe the transformation behavior of the grains at constant composition. The reversibility of the transformation is a further indication of an isochemical process. The phases present were identified by selected-area electron diffraction, enabling diffraction patterns to be recorded from regions of 1000Å in size.

RESULTS

The transformation behavior of synthetic mooihoekite, $\text{Cu}_6\text{Fe}_9\text{S}_{16}$

The observations described below were made on sample 414 synthesized by Cabri (1973). Electron-microscope observations made on the material before heating showed that, although it appeared to be single-phase in both reflected light and X-ray powder photographs (Cabri 1973), the material is in fact two-phase, consisting of a coherent intergrowth of lamellae of a $P42m$ phase in a matrix of the $I43m$ phase. For convenience, the phases present will be referred to by their space groups. Observations over a

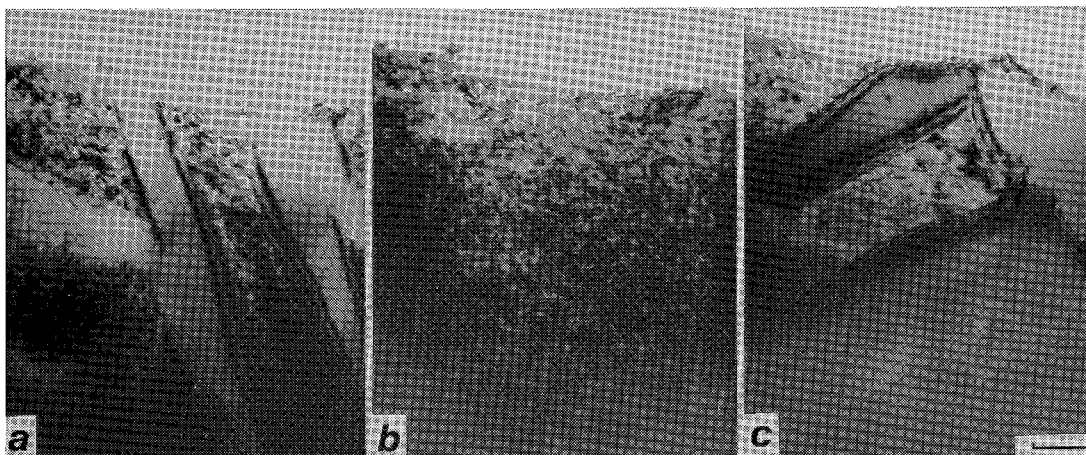


FIG. 2. (a) Transmission electron micrograph of a typical sample of specimen 414. The lamellar phase has the $P\bar{4}2m$ mooihoeckite structure whereas the matrix has the $I43m$ talnakhite structure. (b) After disordering and then cooling, the whole grain has the $I43m$ structure. (c) After a second disordering-reordering cycle, but with a slower cooling rate, the grain contains both phases. Different proportions of the two phases can be formed by varying the cooling rate. Scale bar represents $0.2 \mu\text{m}$.

large number of grains indicate that the sample contains about 60% of the $P\bar{4}2m$ phase. Electron-diffraction patterns taken of such two-phase regions show no splitting of reflections, and as the tetragonal phase exists in all possible twin-related orientations, such a coherent intergrowth would be impossible to detect by X-ray diffraction. Figure 2a shows a typical sample of this material prior to the heating experiments. Note the perturbed nature of the $I43m$ structure.

This two-phase material disorders in stages on heating. The $I43m$ phase transforms to a $P\bar{4}3m$ phase (see below) prior to completely disordering to the $F\bar{4}3m$ phase. The $P\bar{4}2m$ lamellae disorder, at a slightly higher temperature, directly to the $F\bar{4}3m$ phase. Complete disorder to the single-phase $F\bar{4}3m$ structure over the whole grain is achieved at around $200^\circ\text{-}250^\circ\text{C}$. The

behavior of this disordered phase on cooling is the same as that described for metal-enriched chalcopyrite (Putnis & McConnell 1976). With very rapid cooling, the $F\bar{4}3m$ phase can be quenched to room temperature. The appearance of partly or fully ordered phases is dependent on the cooling rate.

The most convenient way of illustrating these transformations is with reference to the schematic Time-Temperature-Transformation (TTT) diagram shown in Figure 3a. In this diagram the onset of a transformation is displayed as a function of temperature and time, and it is therefore important to realize that it describes thermodynamically irreversible behavior. It can be considered as a non-equilibrium phase diagram representing phase changes as a function of thermal history.

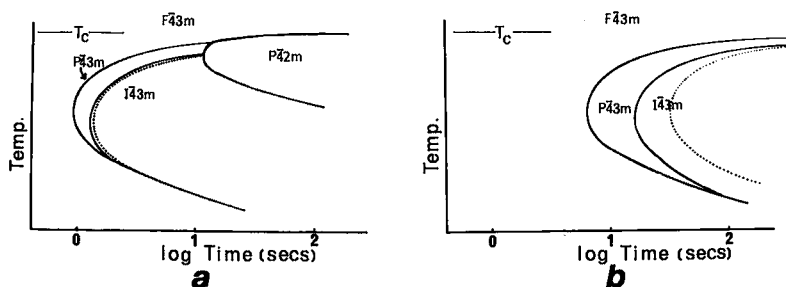


FIG. 3. (a) Schematic TTT plot illustrating the transformation behavior for natural and synthetic mooihoeckite. (b) A similar diagram for natural talnakhite. The dotted curves in both diagrams show the onset of modulation in the $I43m$ structure.

In a thermally activated process the TTT curve has the characteristic C-curve shape, as the transformation rate depends on the thermodynamic driving force ΔG and the diffusion coefficient D . At small degrees of undercooling ΔG is small and D is large, whereas at low temperatures ΔG is large and D is small. The optimum degree of undercooling for which the transformation rate is a maximum corresponds to the 'nose' of the C-curve. TTT diagrams are described by Chadwick (1972), and their application to mineralogical systems has been outlined by McConnell (1975) and Champness & Lorimer (1976).

To a first approximation such diagrams can be used to predict the transformation sequence at a given cooling rate, as a superimposed cooling curve will indicate whether or not a particular phase transformation will occur. Strictly speaking, however, they describe the time and temperature required for an isothermal transformation.

Experimentally, TTT curves are derived by quenching to a particular temperature followed by an isothermal anneal. In the present work, however, owing to the uncertainty of the temperatures of the grains in the *in situ* experiments, Figures 3a, b were derived from heating and cooling experiments which defined the relative positions of the C-curves for the phases observed. In that sense the diagrams are schematic, but they are an accurate description of the relationship between the phases and are consistent with all the experimental results.

Figure 3a shows that the $P\bar{4}2m$ phase will form directly from the disordered phase on slow cooling, but that on more rapid cooling, the transformation involves the formation of two metastable phases: firstly, the $P\bar{4}3m$ phase (with a cell edge equal to that of the $F\bar{4}3m$ phase), and secondly, the $I\bar{4}3m$ phase. Over a fairly wide range of cooling rates the $I\bar{4}3m$ phase is the end result of the transformation sequence and at room temperature no further transformations occur, effectively stranding this metastable phase.

Figure 2b shows the grain after disordering and cooling. This microstructure is characteristic of the $I\bar{4}3m$ phase which exists in this case over the whole grain. Figure 2c shows the result of a further heating and cooling cycle on this grain, in which the cooling was carried out over a longer period to enable the nucleation of the $P\bar{4}2m$ phase. Almost the whole of the grain has transformed to the $P\bar{4}2m$ structure, coherently intergrown with the stranded $I\bar{4}3m$ phase. Different proportions of the two phases can be obtained by varying the experimental cooling rate, illustrating that both phases have the same or

very similar composition in this case. The problem of converting the entire grain to the $P\bar{4}2m$ phase is discussed in the next section.

Transformation from the $I\bar{4}3m$ phase to the $P\bar{4}2m$ phase occurs by annealing below the disordering temperature. The nature of this transformation, which can proceed by two different mechanisms, provides a fundamental insight into the relationship between the two phases. The $P\bar{4}2m$ phase can either nucleate and grow coherently within the $I\bar{4}3m$ phase, producing a microstructure as shown in Figure 2c, in which the $P\bar{4}2m$ lamellae form in twin-related orientations, or the modulated structure characteristic of the $I\bar{4}3m$ phase can progressively coarsen until it exceeds a critical value and proceed to convert the entire grain to twinned $P\bar{4}2m$ phase. Figure 4 a-d illustrates the second transformation sequence in synthetic mooihoekite. Further details of these two mechanisms are in Putnis & McConnell (1976). The significance of this sequence is that it characterizes the modulated nature of the $I\bar{4}3m$ structure in terms of an attempted transformation to the stable $P\bar{4}2m$ phase, confirming the metastability of the $I\bar{4}3m$ phase in relation to the $P\bar{4}2m$ structure.

A large number of such heating experiments has been performed and many disordering-reordering cycles carried out under differing cooling rates in order to construct the TTT diagram in Figure 3a. The ease of formation or *accessibility* of the phases in terms of the relative kinetics of the transformations can be described with reference to this diagram.

The transformation behavior of natural mooihoekite

Electron microscope observations of unheated natural mooihoekite show that again both the $I\bar{4}3m$ phase and the $P\bar{4}2m$ phase are present in the sample, although the $P\bar{4}2m$ phase predominates. Fine intergrowths of "haycockite-type minerals" (with superstructures involving a factor of 3) are also present in the apparently single-phase mooihoekite. Single-phase grains can be found, however, and their transformation behavior is the same as that described for the synthetic sample, although one additional observation is worthy of mention. This concerns the nucleation and growth of the $P\bar{4}2m$ phase on cooling from the disordered form.

When a single-phase grain of the $P\bar{4}2m$ structure is heated it transforms directly to the disordered form. On cooling at a rate appropriate to the formation of the $P\bar{4}2m$ phase, nucleation and growth occur in much the same way as shown in Figure 2c. The result is an inter-

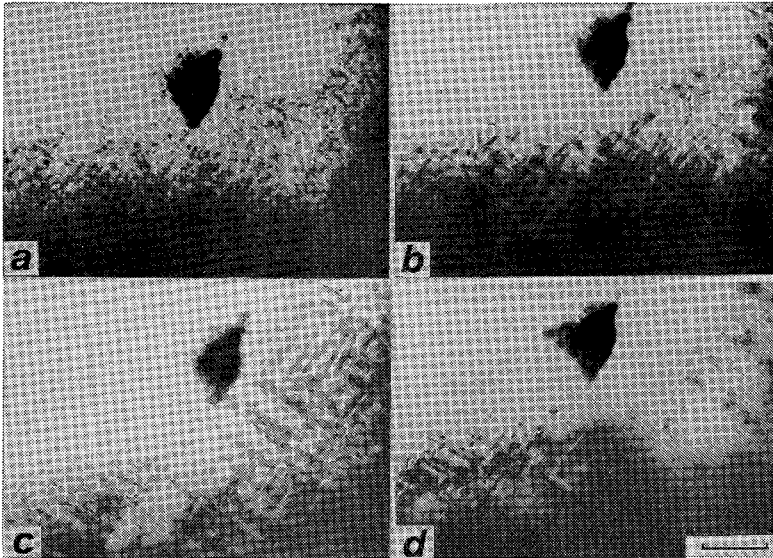


FIG. 4. The process of transformation from (a) the $I\bar{4}3m$ structure to (d) the $P\bar{4}2m$ structure by progressive coarsening. The specimen is synthetic (414), and the total annealing time from a-d is 50 seconds at a temperature just below the disordering temperature. Scale bar represents $0.2 \mu\text{m}$.

growth of the $P\bar{4}2m$ and $I\bar{4}3m$ phases. However, it is generally not possible to transform the whole grain back to the $P\bar{4}2m$ structure, as the volume of the phase formed is controlled by the coherency strains associated with the intergrowth. As the coherent lamellae grow, the magnitude of the elastic energy is proportional to their volume; thus ultimately growth will stop unless dislocations form at the interface, reducing the elastic energy and replacing it with a surface energy. The introduction of these interface dislocations, however, requires an activation energy, and therefore a barrier exists between the growth of the coherent phase up to a certain critical volume, and the completion of the transformation which involves loss of coherency. In these *in situ* experiments, loss of coherency was not observed; indeed, considering that the free-energy difference between the partly ordered and ordered phases is likely to be small, the kinetics associated with the loss of coherency may be such that the complete transformation to the $P\bar{4}2m$ structure is not achieved even over long periods. The presence of the $I\bar{4}3m$ structure in apparently single-phase synthetic mooihoekite that had been annealed at 100°C for 25 days (Cabri 1973) supports this conclusion.

The transformation behavior of talnakhite

Electron microscope observations of unheated talnakhite from Noril'sk show that it has the modulated microstructure characteristic of the $I\bar{4}3m$ phase. Figure 5 shows the typical microstructure of natural talnakhite. This microstructure is highly significant in the interpretation of the nature of this phase, a point which will be taken up later. Commonly, small coherent lamellae (approximately $0.1\text{--}0.2 \mu\text{m}$ long) of chalcopyrite can be seen to have nucleated within the talnakhite, and any interpretation of the probe analyses in Figure 1 must be made bearing this in mind.

On heating, the modulation is lost, and there is a temperature interval over which the $I\bar{4}3m$ structure exists without the modulation. At a slightly higher temperature a transformation to the $P\bar{4}3m$ phase occurs, just prior to complete disordering and the formation of the $F\bar{4}3m$ phase. The temperature for disordering is similar to that for the $P\bar{4}2m$ natural mooihoekite. On cooling, this transformation sequence is reversed, but the rates at which the ordering processes occur are many times slower than the equivalent transformations in natural and syn-

DISCUSSION

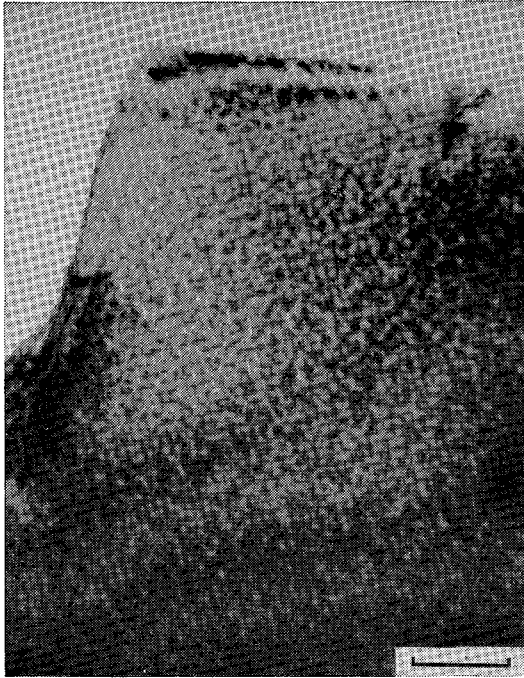


FIG. 5. Electron micrograph of talnakhite from Noril'sk showing the typical modulated microstructure characteristic of the $I\bar{4}3m$ phase. Scale bar represents 0.2 μm .

thetic mooihoeikite. This can be seen by comparison of the schematic TTT diagram for talnakhite (Fig. 3b) with that of mooihoeikite (Fig. 3a). After the initial formation of the $P\bar{4}3m$ phase on cooling, the $I\bar{4}3m$ phase develops relatively sluggishly, and exists initially without any modulation. The modulation develops on slower cooling or on annealing. The development of this modulation is a clear indication of a further attempt at transformation from the $I\bar{4}3m$ structure, and the transformation behavior observed in mooihoeikite shows that the $P\bar{4}2m$ structure is the end result of this process. In natural talnakhite, however, the kinetics of the transformations are such that the $P\bar{4}2m$ phase could not be obtained by the *in situ* experiments and the $I\bar{4}3m$ phase remains stranded. The persistence of the modulated structure in natural material suggests that the $P\bar{4}2m$ phase is kinetically unattainable at low temperatures over long periods of time at these compositions. This leads to the apparent separation of the compositional phase fields for the talnakhite and mooihoeikite structures.

The transformation behavior described here confirms the earlier results of Putnis & McConnell (1976): the formation of partly ordered and ordered phases in this part of the Cu-Fe-S system is governed by the kinetics of the processes involved, and suggests that the $I\bar{4}3m$ structure of talnakhite should not be tied to a strict stoichiometry, nor should it be considered without reference to its attempted transformation to the $P\bar{4}2m$ structure of mooihoeikite. The relative rates of the processes as a function of composition establish that there will be compositional restrictions on the accessibility of the two phases. This can be illustrated by changes in their relative phase fields on a TTT diagram.

The problem of dealing with a system of this kind, in which alternative metastable behavior (McConnell 1975; Putnis 1976) occurs, is firstly, to recognize the metastable and stable behavior, and secondly, to explain why certain states are easier to nucleate, *i.e.*, more accessible than others. In sulfides, where dynamic observations of phase transformations are possible, a study of the transformation behavior as a function of temperature and time can provide, under favorable conditions, an answer to the first problem. The importance of the microstructure in this context makes transmission electron microscopy an ideal tool for this purpose. The second problem requires a theoretical consideration of the symmetry changes associated with possible transformations, and hence of the constraints on the processes involved. Such a theory has been developed by McConnell (1977), based on the group theoretical approach used originally by Landau & Lifshitz (1958), and can be directly applied to this system. Both the theoretical and the experimental aspects must be considered together to provide a more complete description of the transformations which have produced the phases observed in natural and experimental systems.

In the theoretical treatment of the problem, the key issue determining the route taken by a transforming species is the accessibility of the possible states of order relative to the free-energy reduction associated with the transformation. In general terms, the accessibility depends on how great are the differences between the two states in an ordering sequence, *i.e.*, on the number of order parameters which must be specified in the transformation. In a transformation from a disordered to a fully ordered state a high degree of specification is required and this will be associated with a greater structural change than in a transformation to a

partly ordered state (e.g., one in which the vacancies are ordered, but cations disordered). Thus the change in space-group symmetry can be used as an indicator of the amount of structural change, the type of transformation and hence the accessibility of the process. In his symmetry-point ordering theory, McConnell (1977) relates the changes in space-group symmetry to one of three possible types of transformations: (A) a second-order transformation involving no nucleation incident, (B) a first-order transformation involving a minor change in structure and symmetry, which is therefore fairly readily accessible (general symmetry-point ordering), and (C) a first-order transformation involving a substantial change in structure and symmetry in which nucleation will generally be difficult. This provides a theoretical basis on which alternative transformation behavior can be discussed.

McConnell (1977) has discussed the application of symmetry-point ordering theory to transformations in metal-enriched chalcopyrite and this is directly relevant to the behavior of talnakhite and mooihokite. The equilibrium transformation from the $F\bar{4}3m$ structure to the $P\bar{4}2m$ structure is of the type C above, which implies a substantial degree of ordering, but a kinetically difficult process. Under conditions of supercooling, this transformation is not accessible and alternative metastable behavior may operate. The transformation from the $F\bar{4}3m$ structure to the $P\bar{4}3m$ structure is, however, of type B, and can be associated with a single aspect of ordering, in this case with the allocation of occupied interstitial sites (Putnis & McConnell 1976). This transformation, as well as being more accessible, does not require a specific stoichiometry, and thus the $P\bar{4}3m$ structure would be expected to be the first-formed structure over a wide compositional range in the intermediate solid solution (*iss*). This is found to be the case, both in this work and in the results of Cabri (1973), who found a primitive cubic phase on quenching a range of compositions in the *iss* field.

The transformation from the $P\bar{4}3m$ structure to the $I\bar{4}3m$ structure is again of type B, implying a further stage in the ordering sequence, associated with a further restriction in composition. The fact that at this stage the structure is still not completely ordered is shown both by its subsequent behavior and by the structural data for this phase (Hall & Gabe 1972). By following the sequence of more accessible transformations, the transforming species is led ultimately to a state of partial order from which nucleation of the stable product becomes progressively less likely as the temperature is decreased. This

situation has been found in a number of other sulfide systems (Putnis 1976).

Thus we have on the one hand the equilibrium behavior which involves the formation of a possibly fully ordered, and hence compositionally restricted structure in a single step, requiring the specification of parameters associated with the ordering of vacancies, Cu and Fe atoms. This substantial change in structure involves a kinetically inaccessible process over a range of compositions and cooling rates. On the other hand, more accessible transformations which increase the degree of order in a stepwise fashion will occur under metastable conditions and produce a series of partially ordered phases over a range of compositions. The behavior of the *iss* should be considered in these terms.

This approach emphasizes the importance of TTT diagrams in the interpretation of solid-state phase transformations in systems where stable equilibrium may not be reached at low temperatures. Considering that high-temperature phase equilibria in a number of important sulfide systems are characterized by the existence of disordered solid solutions, a reappraisal of the methods used to study their behavior on cooling may be required. In many cases, the traditional sealed silica-tube experiments will not be satisfactory, and in cases such as the *iss*, with the possibility of complex coherent intergrowths, X-ray diffractometry is not sufficient in the identification of the phases present. The electron microprobe also may have severe limitations in describing the compositions of apparently single-phase materials in a system where the balance between thermodynamically ideal behavior and kinetic accessibility leads to a multiphase, metastable assemblage. In such a system the transmission electron microscope should be regarded as a routine instrument in the identification of phases in experimental runs, and *in situ* studies of transformation behavior may provide some insights into the nature of the processes which lead to such complex assemblages.

CONCLUSIONS

1. Talnakhite has a metastable structure in relation to a transformation to the mooihokite structure.
2. The talnakhite structure has a broad range of possible compositions including both $\text{Cu}_9\text{Fe}_8\text{S}_{16}$ and $\text{Cu}_6\text{Fe}_6\text{S}_{16}$.
3. The relatively restricted compositions found for natural talnakhite are the result of a change in kinetics of the ordering transformations with composition.

4. The ordering transformations can be described in terms of the symmetry-point ordering theory which provides a theoretical basis for the observed kinetics.

5. Ordering transformations in sulfide solid solutions should be considered in terms of the accessibility of both stable and metastable phases.

ACKNOWLEDGEMENTS

I would like to thank Dr. L. J. Cabri for his cooperation and provision of the samples, without which this study would not have been possible. I am grateful to Dr. J. D. C. McConnell for many discussions during the course of this work and to the Natural Environment Research Council for the provision of a Research Fellowship.

REFERENCES

- CABRI, L. J. (1967): A new copper-iron sulfide. *Econ. Geol.* **62**, 910-925.
- (1973): New data on phase relations in the Cu-Fe-S system. *Econ. Geol.* **68**, 443-454.
- & HALL, S. R. (1972): Mooihoekite and haycockite, two new copper-iron sulfides, and their relationship to chalcopyrite and talnakhite. *Amer. Mineral.* **57**, 689-708.
- & HARRIS, D. C. (1971): New compositional data on talnakhite. *Econ. Geol.* **66**, 673-675.
- CHADWICK, G. A. (1972): *Metallography of Phase Transformations*. Butterworths, London.
- CHAMPNESS, P. E. & LORIMER, G. W. (1976): Exsolution in Silicates. In *Electron Microscopy in Mineralogy* (H.-R. Wenk, ed.). Springer-Verlag, Berlin Heidelberg New York.
- HALL, S. R. (1975): Crystal structures in the chalcopyrite series. *Can. Mineral.* **13**, 168-172.
- & GABE, E. J. (1972): The crystal structure of talnakhite, $\text{Cu}_{18}\text{Fe}_{10}\text{S}_{32}$. *Amer. Mineral.* **57**, 368-380.
- & ROWLAND, J. F. (1973): The crystal structure of synthetic mooihoekite, $\text{Cu}_9\text{Fe}_5\text{S}_{16}$. *Acta Cryst.* **B29**, 579-585.
- HILLER, J. E. & PROBSTHAIN, K. (1956): Thermische und röntgenographische Untersuchungen am Kupferkies. *Z. Krist.* **108**, 108-129.
- KANDIAH, K., SMITH, A. J. & WHITE, G. (1975): A pulse processor for X-ray spectrometry with Si(Li) detectors. Paper 2.9 2nd ISpra Nuclear Electronics Symposium, Stresa, Italy.
- LANDAU, L. D. & LIFSHITZ, E. M. (1958): *Statistical Physics*. Addison Wesley, Reading, Mass.
- MCCONNELL, J. D. C. (1975): Microstructure of minerals as petrogenic indicators. *Ann. Rev. Earth Planetary Sci.* **3**, 129-155.
- (1977): *K*-space symmetry rules and their application to ordering behavior in non-stoichiometric (metal-enriched) chalcopyrite. *Phys. Chem. Minerals* (In press).
- PUTNIS, A. (1976): Alternative transformation behavior in sulfides: direct observations by transmission electron microscopy. *Science* **193**, 417-418.
- & MCCONNELL, J. D. C. (1976): The transformation behaviour of metal-enriched chalcopyrite. *Contr. Mineral. Petrology* **58**, 127-136.
- ROWLAND, J. F. & HALL, S. R. (1975): Haycockite, $\text{Cu}_4\text{Fe}_5\text{S}_8$: a superstructure in the chalcopyrite series. *Acta Cryst.* **B31**, 2105-2112.
- STATHAM, P. J. (1976): A comparative study of techniques for quantitative analysis of the X-ray spectra obtained with a Si(Li) detector. *X-ray Spectrometry* **5**, 16-28.

Received June 1977; revised manuscript accepted September 1977.